

## INVESTIGATION OF ELECTRON RELAXATION IN BISMUTH BY THE CYCLOTRON RESONANCE TECHNIQUE

S. M. CHEREMISIN, V. S. ÉDEL'MAN, and M. S. KHAÏKIN

Institute of Physics Problems, USSR Academy of Sciences

Submitted April 21, 1971

Zh. Eksp. Teor. Fiz. **61**, 1112–1119 (September, 1971)

The relaxation time  $\tau$  of light conduction electrons in bismuth is measured by the cyclotron-resonance technique in the frequency range from 10 to 135 GHz and at temperatures between 0.35 and 4.2°K. The dependence  $\tau^{-1} \propto K(f)T^2 + \tau^{-1}(f)$  is found. The functions  $K(f)$  and  $\tau^{-1}(f)$  have singularities at a frequency  $f \approx 50$  GHz, at which the cyclotron-frequency phonon momentum is equal to the diameter of the electron Fermi surface. This means that electron-phonon interaction predominates in electron relaxation. The experiments are in agreement with the simplified theory of the phenomenon. The residual relaxation time in the investigated bismuth single crystals is 1–2 nsec for light electrons and 4–6 nsec for holes.

**T**HE use of cyclotron resonance (CR) for the study of carrier relaxation processes due to electron-electron and electron-phonon interactions<sup>[1]</sup> in metals has the following advantages over dc measurements of the carrier mobilities:

1. Since different carrier groups have different effective masses, measurement of the width of the CR line makes it possible to measure directly the relaxation time  $\tau$  for each of the groups separately.

2. The electron excitation energy above the Fermi level is, at sufficiently low temperatures ( $kT < \hbar\omega$ ), of the order of  $\hbar\omega$ , where  $\omega$  is the frequency of the external electromagnetic field; the scattering occurs in this case with practically constant change of the electron energy  $\Delta E \sim \hbar\omega \sim \hbar\omega_c$  ( $\omega_c$  is the cyclotron frequency), and this simplifies the analysis of the results.

3. For high-grade crystals at sufficiently high frequencies, scattering by impurities and defects has little influence on the relaxation time, which is determined even at very low temperature mainly by the interaction of the elementary excitations.

The electron-relaxation mechanism in bismuth has not been explained to this day. It is proposed in<sup>[2,3]</sup> that the main contribution to the scattering in an ideal crystal is made by electron-electron interaction. Electron-phonon scattering is assumed in<sup>[4,5]</sup>. We have investigated experimentally the relaxation times of the electrons in bismuth in the frequency range 10–135 GHz, and established that the main contribution to the scattering is made by electron-phonon interaction.

### EXPERIMENT

The samples were single crystals of bismuth with normal N parallel to the trigonal axis  $C_3$  and were grown from the melt in a dismountable quartz mold.<sup>[6]</sup> The raw material was bismuth of "experimental" grade produced by Giredmet (State Institute for Rare Metals). The residual free-path time bounded by scattering by impurities and crystal defects was 1–2 nsec for light electrons and 4–6 nsec for holes. A change of temperature from 4.2 to 1.5°K was effected by pumping off <sup>4</sup>He vapor, and a reduction to 0.35°K was produced by pump-

ing off <sup>3</sup>He vapor. The resonators with the sample were placed in a vacuum-type screen, into which the heat-exchange gas (<sup>4</sup>He or <sup>3</sup>He) was admitted during the time of the experiment up to a pressure  $\sim 10$  Torr at room temperature.

The surface resistance was measured with a direct-amplification spectrometer with a flow-through resonator, one of the walls of which was the sample. The signal from a klystron or from a backward-wave tube was frequency-modulated, passed through the resonator, and detected. The modulation frequency ranged from 1 to 5 kHz, and the modulation amplitude was such that the frequency deviation was several times larger than the bandwidth of the resonator. The signal from the microwave detector, which duplicated the form of the resonance curve, was amplified by a broadband amplifier and passed through a peak detector and a selective amplifier with a synchronous detector. The output of the latter was a signal of 12 Hz frequency produced by modulating the magnetic field applied to the sample at this frequency. The large frequency deviation of the microwave generator made it possible to operate without an automatic frequency control system, since the fluctuations of the generator frequency influenced only the phase but not the amplitude of the signal fed to the peak detector.

At wavelengths shorter than 8 mm, the microwave detector was a bolometer based on an Allen-Bradley resistor or made of an InSb crystal with a volume no larger than 1 mm<sup>3</sup>. The detector was coupled to the resonator directly, through an aperture in the wall of the latter, without an intermediate waveguide. Such detectors have a sensitivity  $10^{-8}$ – $10^{-9}$  W at an amplifier bandwidth  $\sim 10$  kHz.

The high sensitivity of the detectors has made it possible to decrease the power dissipated in the resonator to  $\sim 10$   $\mu$ W, which is necessary when working with <sup>3</sup>He. In this case the heat rise of the sample relative to the helium bath did not exceed several hundredths of 1°K. In all the experiments, the power dissipated in the resonator was low enough to keep the sample from overheating: no change in the CR line width was observed when the power was changed by several times.

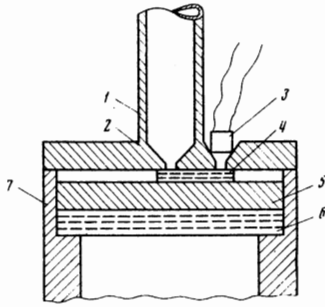


FIG. 1. Measuring resonator for the 2 mm band: 1—input waveguide, 2—mirror, 3—detector, 4—quartz disk, 5—sample, 6—quartz substrate, 7—sample holder.

Strip resonators<sup>[7]</sup> were used at frequencies 10–37 GHz, and cavity resonators of different constructions were used at higher frequencies. At 135 GHz we used a resonator (Fig. 1) made up of a half-wave segment of a dielectric waveguide (fused-quartz disk of 4.5 mm diameter) short-circuited by metal mirrors;<sup>[8]</sup> one of the mirrors was the sample. The  $Q$  of such a resonator is  $\sim 1500$  and is determined mainly by the loss in the sample.

The reflections from the elements of the microwave channel, the length of which was  $(10^2-10^3)\lambda$ , made the circuit sensitive to changes not only of the resonator  $Q$  but also of its natural frequency, and therefore the signal registered at the output of the measuring circuit was

$$U \sim a\partial R / \partial H + b\partial X / \partial H, \quad (1)$$

and was governed by changes of both the surface resistance  $R$  and the surface reactance  $X$  of the sample.

The magnetic field was produced by a system of Helmholtz coils, and the homogeneity of the field in the volume of the sample was no worse than 0.1%. When working in fields  $< 100$  Oe, the earth's magnetic field was cancelled out.

We measured the relaxation time of the electrons with minimum mass ( $m^*/m_0 = 0.0094$ ) in a field  $H$  parallel to the binary axis  $C_2$ . We usually observed the CR of electrons belonging to two ellipsoids of the Fermi surface. If the direction of the high-frequency currents was at an angle  $30^\circ$  to the magnetic field, then CR was observed from only one of the ellipsoids; in this case, no line splitting takes place when the field is rotated in the basal plane through a small angle away from the  $C_2$  direction. When the angle between  $H$  and  $C_2$  was less than  $15^\circ$ , the relative width of the CR line remained constant within the limits of measurement accuracy. With further increase of the angle between  $H$  and  $C_2$ , the mutual superposition of the CR lines corresponding to different effective masses for the three Fermi-surface ellipsoids made it difficult to analyze the plots, and the line width was not measured under such conditions.

In the measurements at 18.74 GHz, when the value of  $\omega\tau$  is maximal, and reaches  $\sim 130$ , it was established that the CR line width is independent of the investigated section of the surface under the strip (its dimensions were  $6.7 \times 2$  mm), of the angle between the magnetic field and the high-frequency current, and of a  $\pm 30'$  tilt of the magnetic field relative to the sample plane. Typical CR plots are shown in Fig. 2.

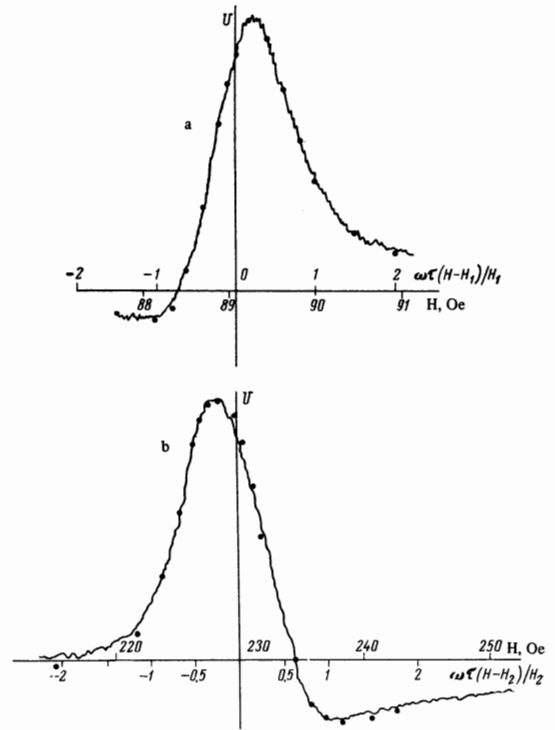


FIG. 2. Cyclotron-resonance lines in bismuth with  $H \parallel C_2$  and  $N \parallel C_3$ : a— $f = 26.4$  GHz, first order,  $T = 0.35^\circ$  K,  $\omega\tau = 114$ ; b— $f = 135$  Hz, second order,  $T = 1.5^\circ$  K,  $\omega\tau = 35$ . Solid line—experimental plot, points—calculation with formula (3).

## RESULTS

To determine  $\omega\tau$  we used the Chambers formula<sup>[9]</sup>

$$Z = (R_0 + iX_0) \left( 1 + \frac{a}{1 - i\mu} \right), \quad (2)$$

where  $R_0$  and  $X_0$  describe the surface impedance far from resonance,  $a \ll 1$ ,  $\mu = \omega\tau(H - H_n)/H_n$ , and  $H_n$  is the CR field of order  $n$ . In the derivation of (2) it was assumed that the mass depends little on the momentum  $p_z$  and that the relative variation of  $R$  and  $X$  at resonance is small; this is practically always the case, and the variation in our experiments did not exceed 15%. For the experimentally observed shape of line (1) we obtain

$$U \sim A \frac{\mu}{(1 + \mu^2)^2} + B \frac{1 - \mu^2}{(1 + \mu^2)^2}. \quad (3)$$

Since the spectrometer registered a mixed signal (1), it is necessary to choose the ratio  $A/B$  such that formula (3) describes the observed line shape.

The only essential condition for the validity of (3) is that the variation of  $Z$  at resonance be small:  $a \ll 1$ . In this case (2) describes the superposition of the wave scattered by the harmonic oscillator and the nonresonant background. Violation of the condition for the anomalous skin effect,  $R \gg \delta$  (where  $R$  is the Larmor radius and  $\delta$  is the depth of the skin layer) leads to a phase change in the nonresonant background and is accounted for automatically, just like the change of the

phase of the impedance with changing frequency at  $V_F/\delta \sim \omega$  ( $V_F$ —Fermi velocity<sup>[10]</sup>), by a suitable choice of  $A/B$  when the plots of the CR line are processed. Thus, the values chosen for  $A/B$  were 1.4 and  $-2$  for the plots in Fig. 2a and Fig. 2b, respectively. The obtained value of  $\omega\tau$  is not very sensitive to this ratio. When the ratio is changed by a factor of 2 the value of  $\omega\tau$  changes by 5%, (in which case the calculated line shape differs considerably from the observed one). For different orders of CR ( $n = 1-3$ ), the relative line width, and consequently also  $\omega\tau$ , is independent of  $n$  within the limits of measurement error.

The temperatures at which the measurements were performed at each frequency are as follows:

Sample:	I	I, II	I	I	II	I	I	II
f, GHz:	10.22	18.74	26.4	37.1	43.7	69.8	98	135
T, °K:	0.35-1.5	0.35-2.5	0.35	0.35-2	1.5	0.35-4.2	1.5	1.5-4.2

The reciprocal relaxation time can be represented in accordance with the measurements (see also Fig. 3 of [1]) in the form

$$\tau^{-1}(f, T) = \tau_0^{-1} + \tau^{-1}(f, 0^\circ\text{K}) + K(f)T^2. \quad (4)$$

A plot of  $K(f)$  is shown in Fig. 3. At 135 GHz, the values of  $\tau(1.5^\circ\text{K})$  and  $\tau(4.2^\circ\text{K})$  differ by only a factor of 1.5, and the measurement accuracy is insufficient to establish reliably the exponent of the  $\tau(T)$  dependence, and therefore the point  $K$  for 135 GHz is not shown in Fig. 3. If we assume that at this frequency, as at the lower frequencies,  $\Delta\tau^{-1} \propto T^2$ , then  $K \approx 1 \text{ nsec}^{-1}\text{deg}^{-2}$ . We note that the values of  $K(f)$  measured at high frequency greatly exceed the value  $K = 0.07 \text{ nsec}^{-1}\text{deg}^{-2}$  obtained in [11] at 10 MHz.

A plot of  $\tau^{-1}(f, 0^\circ\text{K})$  is shown in Fig. 4. The values of  $\tau^{-1}(f, 0^\circ\text{K})$  were obtained by extrapolating the measured values of  $\tau$  to  $T = 0^\circ\text{K}$  in accordance with the data of Fig. 3. The values of  $\tau$  measured at  $T = 0.35^\circ\text{K}$  practically coincide with those obtained by extrapolation. At 43.7, 98, and 135 GHz, the extrapolation was carried out in accordance with the law  $\Delta\tau^{-1}[\text{nsec}^{-1}] = T^2[\text{deg}^2]$ ; the correction obtained in this manner,  $[\tau^{-1}(1.5^\circ\text{K}) - \tau^{-1}(0^\circ\text{K})]/\tau^{-1}(0^\circ\text{K})$ , did not exceed 20%. The parameter  $\tau_0^{-1}$  for sample I was determined by extrapolating the initial section ( $f \lesssim 40$  GHz) of the  $\tau^{-1}(f, 0^\circ\text{K})$  dependence in accordance with the law  $\tau^{-1}(f, 0^\circ\text{K}) \propto f^3$  and turned out to equal  $0.65 \text{ nsec}^{-1}$ . For sample II, the value of  $\tau^{-1}$  was determined by comparison with sample I at 18 GHz:

$$\tau_{0II}^{-1} = \tau_{0I}^{-1}(18 \text{ GHz}, T) - \tau_I^{-1}(18 \text{ GHz}, T) + \tau_{0I}^{-1} = 1 \text{ nsec}^{-1}.$$

**DISCUSSION**

Let us examine a simplified model of the electron-phonon relaxation process for first-order CR, neglecting the anisotropies of the phonon spectrum and of the electron ellipsoid in the plane perpendicular to its major axis.

At  $kT \ll \hbar\omega_C$  the main process of relaxation of the excited electrons will be the spontaneous emission of phonons of frequency  $\omega_C$ . The probability of emitting longitudinal phonons can be written in the form<sup>[12]</sup>

$$P \sim \omega(1 - F)V(\omega), \quad (5)$$

where  $(1 - F)$  is the density of the unoccupied states on

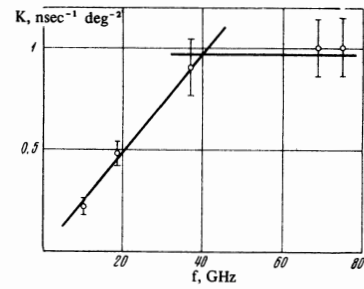


FIG. 3. Frequency dependence of the coefficient  $K$  at  $T^2$  in (4). The bars at the points represent the measurement errors.

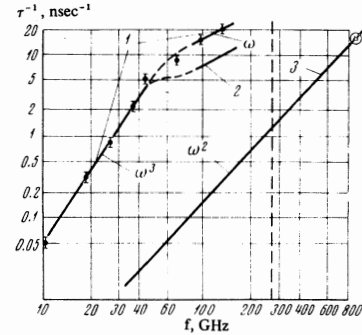


FIG. 4. Frequency dependence of  $\tau^{-1}(f, 0^\circ\text{K})$ . The bars at the points represent the measurement errors. Lines 1 and 2—calculation in accord with the anisotropic and isotropic models, respectively; dashed line—limit of applicability of the model; 3—frequency dependence of the electron-electron scattering in accordance with the data of [3].

the Fermi surface and  $V(\omega)$  is the phase volume of the phonons of frequency  $\omega$ , determined by the momentum conservation law. We can regard  $1 - F$  as independent of the magnetic field, neglecting by the same token the quantum oscillations of the relaxation time.

From the point O (Fig. 5) the electron can be scattered to points lying on the line at which the Fermi surface, which differs little from a cylinder near the central section, intersects the phonon sphere of radius  $\hbar\omega_C/v$  ( $v$  is the isotropic speed of sound)—curve A on Fig. 5. Since the electron executes many ( $\sim \omega\tau$ ) revolutions along the trajectory between the scattering acts, the states allowed for the scattered electrons lie on the surface obtained by revolving the curve A around the  $z$

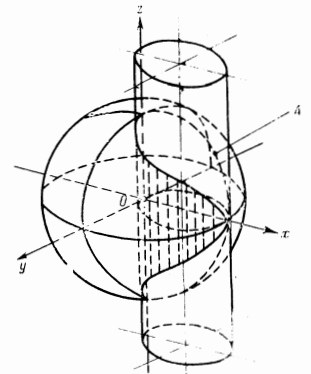


FIG. 5. Diagram illustrating the scattering of electrons at  $f \approx 50$  GHz;  $z$ —major axis of electron ellipsoid of Fermi surface. Sphere radius  $p = \hbar\omega_C/v$ . The states allowed for the electrons scattered from the point O lie on the Curve A.

axis; this surface is part of the surface of a sphere of radius  $\hbar\omega_c/v$ , contained inside a cylinder whose radius is equal to double the Fermi momentum of the electrons of the central section. The phase volume  $V(\omega)$  is proportional to the area of this surface. The average diameter of the electron ellipsoid is  $13 \times 10^{-21}$  g-cm-sec<sup>-1</sup>,<sup>[13]</sup> and the momentum of a longitudinal phonon of frequency  $f$  is equal to  $2.8 \times 10^{-31}$  f [g-cm-sec<sup>-1</sup>].<sup>[14]</sup> The sphere becomes tangent to the cylinder (Figure 5 corresponds to this case) at  $f \approx 50$  GHz, and then the volume  $V(\omega)$  is maximal and double its asymptotic value at  $f \gg 50$  GHz. The behavior of  $V(\omega)$  near  $f = 50$  GHz depends strongly on the exact form of the central section of the Fermi surface and on the anisotropy of the velocity of sound.

Figure 4 shows plots of  $\tau^{-1}(f, 0^\circ\text{K})$ , obtained from formula (5) (accurate to a constant factor) at  $f \lesssim 50$  GHz and  $f \gtrsim 100$  GHz. Curve 2 was plotted under the assumption that the scattering probability is isotropic, and in plotting curve 1 we took into account the fact that at large  $\omega$  the phonons are emitted predominantly at small angles to the major axis of the ellipsoid, and the probability of interaction is approximately twice as large as when the phonon is emitted along the binary axis.<sup>[14]</sup>

Scattering by transverse phonons ( $p \approx 6 \times 10^{-31}$  f [g-cm-sec<sup>-1</sup>]) can lead to singularities of  $\tau(f)$  near  $f = 20$  GHz. To observe this effect it is necessary to perform measurements at lower frequencies, calling for the use of samples with a residual relaxation time 10–20 nsec, i.e., larger by one order of magnitude than the  $\tau_0 = 1\text{--}2$  nsec of our samples. It is still not clear how to improve the crystal quality further, all the more since the samples obtained by other methods (for example, by electric-spark finishing with subsequent etching) give results that are still worse by one order of magnitude.<sup>[3]</sup>

At  $kT \sim \hbar\omega$  it is necessary to introduce in (5) terms describing the absorption and induced emission of phonons. In the range  $kT/\hbar\omega = 0.3\text{--}3$ , the Bose-Einstein distribution function differs from a parabola  $(kT/\hbar\omega)^2$  by not more than 10%; therefore experiment should reveal a dependence in the form  $\tau^{-1}(T) - \tau^{-1}(0^\circ\text{K}) \propto V(\omega)T^2/\omega$ , which is a good agreement with the data of Fig. 3. At  $kT \gg \hbar\omega$ , the characteristic energy of the electron excitation above the Fermi level becomes equal to  $kT$  and the expected dependence is apparently  $\tau^{-1} \propto T^3$ . The relative CR line width, however, is thereby increased so appreciably that a determination of the relaxation time with any degree of accuracy is impossible.

The absolute magnitude of electron-phonon damping at the frequencies of our experiments can be compared with the results of a calculation<sup>[4]</sup> of the relaxation time at  $T = 20^\circ\text{K}$ , in which an isotropic deformation potential was used; the value obtained in<sup>[4]</sup> is  $\tau \approx 5 \times 10^{-11}$  sec. Extrapolation of curve 1 of Fig. 4 to  $f = 270$  GHz, corresponding to  $T = \hbar\omega/k = 13^\circ\text{K}$ , yields  $\tau = 2 \times 10^{-11}$  sec, i.e., the order of magnitude of the observed values of  $\tau$  agrees with the known values of the deformation potential.<sup>[14]</sup> An exact calculation of the electron relaxa-

tion time in bismuth in accordance with the known deformation-potential tensor, with allowance for anisotropy, is rather cumbersome and has not been performed to date.

At 270 GHz, the phonon momentum becomes comparable with the maximum Fermi momentum of the electrons, and the model under consideration is no longer valid for high frequencies. In addition, at frequencies above 300 GHz it is necessary to take into account the quantum oscillations of the relaxation time, with amplitude  $\hbar\omega/E_F$ . It is probable that in this frequency region the electron-phonon scattering is sharply decreased (since it is impossible to satisfy simultaneously the energy and momentum conservation laws in the single-phonon process), making it possible to observe the electron-electron scattering; the latter, according to<sup>[3]</sup> (see Fig. 4) makes a negligibly small contribution to the relaxation time in the frequency region  $f < 300$  GHz.

In conclusion we must emphasize the following: the character of the  $\tau^{-1}(\omega, T)$  dependences, and particularly the presence of a kink on the  $\tau^{-1}(\omega)$  curve near the frequency at which the phonon momentum becomes comparable with the Fermi-surface diameter, allows us to state that the main process determining the scattering of electrons in bismuth in the investigated frequency region is electron-phonon interaction.

The authors are grateful to P. L. Kapitza for interest in the work, to I. Ya. Krasnopolin and V. M. Pudalov for useful discussions, to M. I. Kaganov, M. P. Kemo-khidze, and L. P. Pitaevskii for a discussion of theoretical questions, and to G. S. Chernyshov for technical help.

<sup>1</sup>V. S. Édel'man and S. M. Cheremisin, ZhETF Pis. Red. 11, 373 (1970) [JETP Lett. 11, 250 (1970)].

<sup>2</sup>E. W. Fenton, J. P. Jan, A. Karlsson, and R. Singer, Phys. Rev. 184, 663 (1969).

<sup>3</sup>H. D. Drew and U. Strom, Phys. Rev. Lett. 25, 1755 (1970).

<sup>4</sup>S. Mase, V. Molnar, and W. Lawson, Phys. Rev. 127, 1030 (1962).

<sup>5</sup>S. M. Bhagat and D. D. Manchon, Phys. Rev. 164, 966 (1967).

<sup>6</sup>M. S. Khaikin, S. M. Cheremisin, and V. S. Édel'man, Pribory i Tekhn. Éksperim. No. 4, 225 (1970).

<sup>7</sup>M. S. Khaikin, *ibid.* No. 3, 95 (1961).

<sup>8</sup>F. J. Rosenbaum, Rev. Sci. Instr. 35, 1550 (1964).

<sup>9</sup>R. G. Chambers, Proc. Phys. Soc. 86, 305 (1965).

<sup>10</sup>R. B. Dingle, Physica 19, 311 (1953).

<sup>11</sup>V. F. Gantmakher and Yu. S. Leonov, ZhETF Pis. Red. 8, 264 (1968) [JETP Lett. 8, 162 (1968)].

<sup>12</sup>J. M. Ziman, Theory of Solids, Cambridge Univ. Press.

<sup>13</sup>M. S. Khaikin and V. S. Édel'man, Zh. Eksp. Teor. Fiz. 47, 878 (1964) [Sov. Phys.-JETP 20, 587 (1965)].

<sup>14</sup>K. Walther, Phys. Rev., 174, 782 (1968).